

Estimating local bonding/antibonding character of canonical molecular orbitals from their energy derivatives. The case of coordinating lone pair orbitals

Patrick Chaquin, Yves Canac, Christine Lepetit, D Zargarian, Rémi Chauvin

▶ **To cite this version:**

Patrick Chaquin, Yves Canac, Christine Lepetit, D Zargarian, Rémi Chauvin. Estimating local bonding/antibonding character of canonical molecular orbitals from their energy derivatives. The case of coordinating lone pair orbitals. International Journal of Quantum Chemistry, 2016, 116, pp.1285 - 1295. 10.1002/qua.25174 . hal-01383238

HAL Id: hal-01383238
https://hal.science/hal-01383238

Submitted on 18 Oct 2016

HAL is a multi-disciplinary open access archive for the deposit and dissemination of scientific research documents, whether they are published or not. The documents may come from teaching and research institutions in France or abroad, or from public or private research centers.

L'archive ouverte pluridisciplinaire **HAL**, est destinée au dépôt et à la diffusion de documents scientifiques de niveau recherche, publiés ou non, émanant des établissements d'enseignement et de recherche français ou étrangers, des laboratoires publics ou privés.

Estimating Local Bonding/Antibonding Character of Canonical Molecular Orbitals from their Energy Derivatives. The Case of Coordinating Lone Pair Orbitals

Patrick Chaquin[1] , Yves Canac[2] , Christine Lepetit[3], Davit Zargarian[4], Remi Chauvin[5]

Correspondance to Patrick Chaquin (E-mail : chaquin@lct.jussieu.fr)

[1]. P. Chaquin
Sorbonne Universités, UPMC Univ Paris 06, CNRS UMR 7616, Laboratoire de Chimie Théorique (LCT), F-75005 Paris, France.

[2] Y. Canac
CNRS, LCC (Laboratoire de Chimie de Coordination), 205, route de Narbonne, BP 44099, F-31077 Toulouse Cedex 4, France.
Université de Toulouse, UPS, INPT, F-31077 Toulouse Cedex 4, France.

[3] C. Lepetit
CNRS, LCC (Laboratoire de Chimie de Coordination), 205, route de Narbonne, BP 44099, F-31077 Toulouse Cedex 4, France.
Université de Toulouse, UPS, INPT, F-31077 Toulouse Cedex 4, France.

[4] D. Zargarian
Département de chimie, Université de Montréal, Montréal (Québec), Canada H3C 3J7

[5]. R. Chauvin
CNRS, LCC (Laboratoire de Chimie de Coordination), 205, route de Narbonne, BP 44099, F-31077 Toulouse Cedex 4, France.
Université de Toulouse, UPS, INPT, F-31077 Toulouse Cedex 4, France.

ABSTRACT.

According to Koopmans theorem, the derivative of the energy of a canonical MO with respect to nuclear coordinates quantifies its bonding/antibonding character. This quantity allows predictions of bond length variation upon ionisation in a panel of 19 diatomic species. In polyatomic molecules, the derivative of a MO energy with respect to a given bond length reveals the nature and the degree of the bonding/antibonding contribution of this MO with respect to this bond. Accordingly, the HOMO "lone pairs" of CO and CN^- and the HOMO-2 of CH_3CN are found to be antibonding with respect to the C-X bond (X = N, O), whereas the HOMO of N_2 is found to be bonding. With the same approach, the variation of the bonding character in the MOs of CO and CH_3CN upon interaction with an electron acceptor (modelled through the approach of a proton) or by applying an electric field was studied.

Introduction

The bonding/antibonding character of a molecular orbital

Several essential concepts in chemistry rely on imperfect definitions, especially regarding quantitative aspects (electronegativity, aromaticity, dativity, etc.). This is also the case of the bonding/antibonding character of molecular orbitals (MOs), which can be appraised by several approaches. According to the IUPAC Gold Book[1] "a bonding (resp. antibonding) molecular orbital is a molecular orbital whose occupation by electrons increases (resp. decreases) the total bonding - usually lowers (resp. increases) the total energy of a molecule. Generally, the energy level of a bonding MO lies lower (resp. higher) than the average of the valence orbitals of the atoms constituting the molecule ". This definition corresponds to a *global* molecular character. The chemist is nevertheless more often interested in a *local* character with respect to a given bond. In this specific purpose, the IUPAC definition can suggests two criteria.

From a theoretical point of view, a MO can be defined to be bonding between atoms A and B when its energy lies below the energy of the AOs from which it is built (definition i). This definition entails the calculation of an "orbital dissociation energy" by computing the mean energy of the both atomic hybrids involved in the MO. [2] Another possible definition (ii) is based on the bond dissociation energy: a MO is said to be bonding between two nuclei A and B if the presence of an electron in this MO increases the dissociation energy D_{AB}. Application of this definition requires that we determine the dissociation energies of both the charge-neutral AB and the cationic species AB^+ resulting from the loss of one electron from the MO in question; in this sense, this approach presents a challenge, theoretically as well as experimentally.

An alternative definition (iii) is based on the force exerted by electrons on nuclei: a MO is considered bonding[a] when the force exerted by the corresponding electron density is attractive

[a] A distinction has been established between "binding " which refers to the force and " bonding " which refers to the energy. In the practice, these both concepts are closely related and only the most familiar term of "bonding" will be used hereafter.

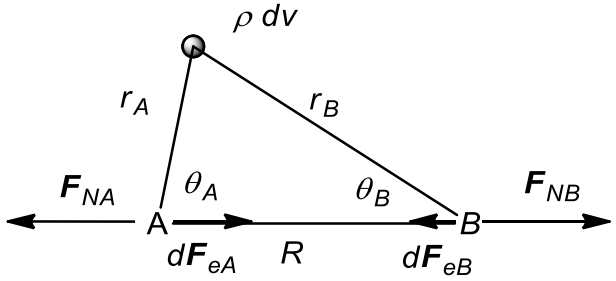
and thus tends to shorten the bond length A-B and *vice versa*. The latter definition will be investigated in the present work. We believe that such an approach is of particular interest for experimentalists because the bonding character of a MO can be correlated to the variation of a number of observable parameters, such as bond length and vibration frequencies, when the corresponding electron is totally (ionization) or partially removed. This is particularly relevant in coordination chemistry where the metal-ligand interaction results in some degree of electron transfer between the ligand and the metal MOs.

Following the Dewar-Chatt-Duncanson model, the bonding in the transition metal complex may be described by the donation from an occupied MO of the ligand to a vacant MO of the metal and back-bonding from an occupied MO of the metal to an empty orbital of the ligand. [3] Indeed, the overlap of MOs of the metal and ligand of suitable energy and symmetry yields a new set of σ or π MOs of bonding, non-bonding or antibonding character in the transition metal complex. The σ MOs normally involve the above-noted donor-acceptor interaction (L→M), whereas the π MOs may involve the same type of interaction or its opposite (namely, π-back bonding, M⇉L). The knowledge of the character of the MOs involved in the metal-ligand interaction (totally or partially bonding/antibonding) may thus allow the rationalization and prediction of the experimental spectroscopic data and/or chemical reactivity of the related complex for which substitution, addition or dissociation, electron transfer reactions, or reaction at coordinated ligands may occur.

Theoretical Basis

Force concept in chemical bonding.

Using the Hellmann-Feynman theorem, Berlin[4] showed that, for a wave function solution of the Schrödinger equation, the force exerted on each nucleus by the other nuclei and by the electrons may be derived in terms of classical electrostatics.



Scheme 1. Electrostatic forces acting in a diatomic molecule AB

In the case of a diatomic molecule AB of internuclear distance *R*, the force F_A on nucleus A is the sum of the (repulsive) force F_{NA} exerted by the other nucleus B (Eq. 1) and the force F_{eA} exerted by the electrons of total density $\rho(x,y,z)$.

$$F_{NA} = F_{NB} = \frac{Z_A Z_B}{R^2} \qquad (1)$$

For symmetry reasons, only the projection of the forces on the nuclear axis AB has to be considered (Scheme 1). The electron force dF_{eA} exerted by the charge ρdv on the nucleus A is attractive (by convention negative) and can be expressed as follows:

$$dF_{eA} = -\left[\frac{Z_A}{r_A^2}\cos\theta_A\right]\rho dv \qquad (2)$$

Similarly, dF_{eb} exerted on the nucleus B is:

$$dF_{eB} = -\left[\frac{Z_B}{r_B^2}\cos\theta_B\right]\rho dv \qquad (3)$$

The electron forces F_{eA} and F_{eB} are equal and can be calculated from Eq. 4 involving the electron density ρ(x,y,z) and the "Berlin function" *f(x, y, z):*

$$F_{eA} = F_{eB} = \int dF_{eA} = \int dF_{eB} = -\frac{1}{2}\int\left[\frac{Z_A}{r_A^2}\cos\theta_A + \frac{Z_B}{r_B^2}\cos\theta_B\right]\rho dv =$$

$$-\frac{1}{2}\int f(x,y,z)\,\rho(x,y,z)dv \qquad (4)$$

The sign of the Berlin function *f(x, y, z)* indicates therefore the bonding or antibonding contribution of an electron density ρ at the point *x*, *y*, *z*: it is bonding if *f* is positive or antibonding if *f* is negative. Thus, for a homonuclear diatomic molecule A_2, a bonding zone ($f > 0$) and an antibonding zone ($f < 0$), separated by a non-bonding nodal surface ($f = 0$) can be defined, as illustrated in Figure 1.

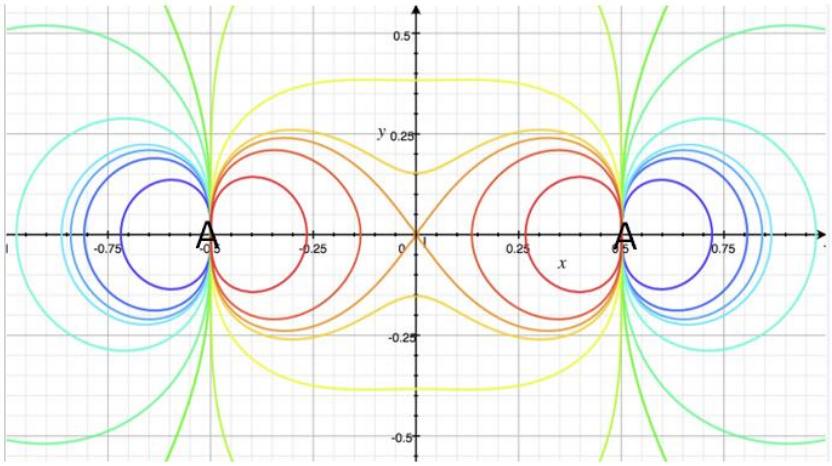


Figure 1. Contour plot of the Berlin function *f*(*x,y,z*) for a diatomic molecule A_2 (red-yellow: bonding zone $f > 0$; green: non-bonding surface $f = 0$; blue: antibonding zone $f < 0$).

For heteronuclear diatomic molecules, the bonding/antibonding zones are reshuffled depending on the ratio Z_A/Z_B. Few examples are given in Figure 2.

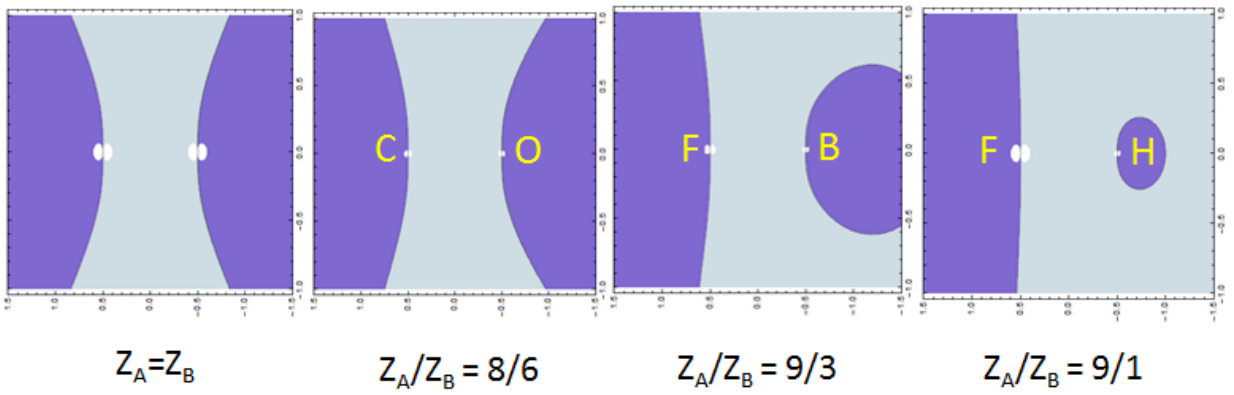


Figure 2. Bonding ($f > 0$, light blue) and antibonding ($f < 0$ dark blue) zones for various Z_A/Z_B values.

The graphs of Figure 2 are very helpful to understand the origin of the usual "visual" identification of bonding or antibonding MOs, only based on the absence/presence of a nodal element cutting the bond. A bonding MO is mainly located in the internuclear region corresponding to strongly positive values of $f(x,y,z)$. On the other hand, if a nodal surface cuts the AB segment, the electron density is repelled out of the bonding region and the MO is likely to be antibonding.

MO energy derivative and (anti)bonding character

From Eq. 1 and Eq. 4, the total force exerted on each nucleus becomes:

$$F = \frac{Z_A Z_B}{R^2} - \frac{1}{2}\int f(x,y,z)\rho dv \qquad (5)$$

Since the total electron density is the sum of occupied spin-orbital densities, the total electronic force can be decomposed into additive orbital forces, following the approach of Bader et al. [5]

Tal and Katriel[6] developed an alternative concept of "orbital forces" which is built up from the MO energy derivatives with respect to nuclear coordinates. Let $E°$ be the Hartree-Fock (HF) energy of a neutral species and E_i^+ the corresponding energy of the cation resulting from the removal of one electron from the i^{th} spin-orbital ϕ_i. According to the generalized Koopmans theorem[7], which assumes that the MOs are the same in the cation as in the original neutral species (approximation of frozen orbitals), the energy ε_i of the i^{th} spin-orbital is:

$$\varepsilon_i = E^0 - E_i^+ \qquad (6)$$

For a diatomic molecule, the derivative with respect to the internuclear distance R yields:

$$\frac{d\varepsilon_i}{dR} = \frac{dE^0}{dR} - \frac{dE_i^+}{dR} \qquad (7)$$

This indicates that the derivative of the MO energy is the difference of the forces acting on nuclei in the presence/absence of an electron in the MO ϕ_i. If the geometry has been taken at its equilibrium value R_e in the neutral species, $dE^0/dR = 0$ and:

$$\left(\frac{d\varepsilon_i}{dR}\right)_{R=R_e} = -\left(\frac{dE_i^+}{dR}\right)_{R=R_e} \qquad (8)$$

According to Eq. 8, if $\varepsilon'_i = d\varepsilon_i/dR$ is positive, R tends to *lengthen* upon loss of an electron in order to *decrease the ion energy* E^+_i, which characterizes a *bonding* ϕ_i MO, in agreement with Mulliken's criterion of the "bonding power" of an electron. [8] Contrary to Bader's orbital forces, the sum of ε'_i over occupied MOs is not equal to the total electronic force: it comes from the fact that the total Hartree-Fock energy is not the sum of the occupied orbital energies. However, the ε'_i forces are more closely related to the Mulliken's criterion. Moreover, they have the advantages of being easily computed by a finite difference of a geometrical parameter, for a diatomic molecule as well as a polyatomic one. Indeed, a similar relation is found with the parameter X associated with any geometrical deformation, involving one or several internal parameters (Eq. 9):

$$\frac{\partial \varepsilon_i}{\partial X} = \frac{\partial E^0}{\partial X} - \frac{\partial E_i^+}{\partial X} \qquad (9)$$

Indeed, there is no certainty that, after MO relaxation and once the correlation energy is taken into account, this "Koopmans' orbital force" ε'_i correctly predicts the actual geometrical variation induced by ionization. Nevertheless one can assume that this quantity reflects a trend which indicates, at least, the sign of this variation. At any rate, this assumption should be validated by comparison with experimental results.

From another point of view, considering that bond elongation destabilizes a bonding MO but stabilizes an antibonding MO, this criterion also agrees with the definition (i) (*vide supra*), provided that the MO energies vary monotonously up to the infinite separation of the atoms, which is generally the case (excluding the cases of endocyclic bonds).

Few works have been devoted to the study of MO energy derivatives in relation to their bonding character. On this basis, Tal and Katriel [6] have determined the bonding character of the MOs of diatomic homonuclear molecules of the Li-F period. Other authors' performed calculations of first and second derivatives of canonical MO energies in some small molecules,[9,10] focussing especially on their geometrical stability[11] (in connection with the Walsh method), or exploring σ and π stabilization in conjugated systems.[12] The slope of orbital energy under geometrical deformation was also used in relation with photoelectron spectra.[13] Because the Kohn-Sham (KS) MOs used in DFT calculations do not obey the Koopmans theorem and thus do not satisfy eq. 7-8, the derivatives of their energies have not the same physical meaning, as demonstrated by Averill and Painter. [14] These authors nevertheless have shown that these quantities can be also used as a bonding criterion and are in qualitative agreement with their HF analogues in Li-F dimers, though rather different in absolute value. They proposed the denomination of "dynamic orbital force" (DOF) for these derivatives, to differentiate them from the additive "static orbital forces" of Bader. More recently, on the same

basis (under the designation of "radial orbital energy slopes"), Bickelhaupt *et al.* performed calculations to determine the bonding character of s-p mixing KS MOs in a set of 6 diatomic molecules.[15] Very recently, finite bond length variations (as "orbital force constants") were used as a measure of the bonding character of KS MOs of few various molecular systems. [16]
In what follows, the idea that the bonding/antibonding character of a given canonical MO can be quantified by the derivative of the MO energy with respect to nuclear coordinates will be developed. These results will then be validated against other classical approaches, previous studies and on the basis of experimental data for a panel of diatomic molecules. They will be extended to HNC, HCN and CH_3CN with a special attention to the hybrid "lone pairs". The bonding/antibonding character of the near-frontier molecular orbitals of well-known infrared spectroscopy probes such as CO and CH_3CN has been indeed debated in the literature.[17] Finally, a range of observable properties will be used to examine the variation of the MO characters of a ligand upon coordination to a charged metal centre; the corresponding perturbations will be mimicked either by a proton approach (a crude description of the ligand (Lewis base) - metal (Lewis acid) interaction), or by applying an electric field.

Methods

All calculations have been performed using the GAUSSIAN09[18] program, at the HF/6-311G** level unless otherwise specified. Derivatives of canonical MO energies ε'_i have been computed numerically using finite difference of +0.002 Å of bond lengths with respect to the equilibrium value at the same calculation level, in order to satisfy Eq. 8. The restricted open HF (ROHF) method has been used for triplet species. For polyatomic molecules, the calculations were performed by variation of one bond length, dragging the separated ends with their original geometry in the equilibrium structure (constant interatomic distances and angles with respect to the head atom). This assumption differs from the one used by Averill and Painter for the definition of DOF.[15]

Unless otherwise indicated, the reported bond lengths R_e and their variations ΔR_e by ionization or protonation (Tables 1, 2 and 6) are experimental values taken from the NIST data bank. When experimental data are not available, high level calculated values were reported from the literature or NIST.

Results and discussion

Homonuclear diatomic molecules

The derivatives of valence shell MO energies of a series of homonuclear diatomic molecules are reported in Table 1. These ε'_i values are in accordance with the expected well-known MO nature, as follows. For instance, in the first period molecules, a large positive ε'_i value (0.164 au) is indeed calculated for the bonding σ_g MO of H_2 in agreement with the H-H bond elongation

from 0.741 Å to 1.053 Å upon removing an electron to give H_2^+. In contrast, a large negative value (-0.275 au) is calculated for the antibonding σ_u MO of He_2. The latter is indeed a very weak Van der Waals complex with R_e = 2.97 Å and, after the loss of an electron from σ_u, the molecular ion He_2^+ with R_e = 1.08 Å is obtained.

Similarly, in molecules of periods 2 and 3, longer bonds result from removal of an electron from bonding MOs in Li_2 ($2\sigma_g$), C_2 ($1\pi_u$) and N_2 ($3\sigma_g$) which exhibit large positive ε'_i values. The reverse holds for F_2, O_2, S_2 and Cl_2 (π_g antibonding in all cases). In the case of P_2, the loss of an electron from the bonding HOMO π_u gives rise to the $^2\Pi_u$ ground state of P_2^+ exhibiting a longer bond than P_2. The case of Ne_2 is very similar to that of He_2: the neutral species is a weak Van der Waals complex with R_e = 3.1 Å, that becomes a molecular ion Ne_2^+ with R_e = 1.75 Å after losing an electron from the antibonding $3\sigma_u$ MO.

Table 1. Energy derivatives ε'_i (au) of valence MOs of homonuclear diatomic molecules (HF/6-311G**); R_e (Å) experimental equilibrium distance; ΔR_e variation of the experimental equilibrium distance (Å) between neutral and cationic species in its ground state; in bold, ε'_i of the MO becoming singly occupied in the cation.

MO	H_2	He_2[a]	MO	Li_2	C_2	N_2	O_2	F_2	Ne_2[b]
$1\sigma_g$	**0.164**	0.305	$2\sigma_g$	0.010	0.190	0.394	0.492	0.343	0.144
$1\sigma_u$		**-0.275**	$2\sigma_u$		-0.137	-0.176	-0.201	-0.167	-0.092
			$3\sigma_g$		-	**0.047**	0.111	0.215	0.131
			$1\pi_u$		**0.122**	0.238	0.209	0.136	0.063
			$1\pi_g$				**-0.199**	**-0.125**	-0.066
			$3\sigma_u$						**-0.216**
R_e	0.741			2.672	1.245	1.098	1.208	1.412	
ΔR_e	0.312			0.37	0.056	0.018	-0.091	-0.090	

Table 1 (continued)

MO	P_2	S_2	Cl_2
$4\sigma_g$	0.115	0.077	0.156
$4\sigma_u$	-0.076	-0.146	-0.063
$5\sigma_g$	-0.008	-0.019	0.096
$2\pi_u$	**0.072**	0.042	0.068
$2\pi_g$		**-0.066**	**-0.056**
R_e	1.893	1.889	1.987
ΔR_e	0.092	-0.064	-0.096

[a] R = 1.0 Å; [b] R = 1.5 Å;

Another interesting issue is the evolution of the $3\sigma_g$ and $5\sigma_g$ MOs of the series. The $3\sigma_g$ MOs have a maximum bonding character in F_2 where the s-p hybridization is weaker, as a result of a large 2s-2p gap in the F atom. This bonding character decreases in the following order $F_2 > O_2 > Cl_2 > N_2 > P_2 > S_2$ which follows the decrease of the s-p gap except for the latter two molecules. In the case of P_2, the $5\sigma_g$ MO can be considered as strictly non-bonding: ε'_i is found slightly negative (-0.008 au) with the 6-311G** basis set but slightly positive (0.001 au) with the cc-pvtz Dunning's basis set. As a matter of fact, in a low lying excited state $^2\Sigma_g$ of P_2^+, resulting from the removal of a $5\sigma_g$ electron from the ground state of P_2, the bond length is 1.893 Å, so unchanged with respect to P_2.

Heteronuclear diatomic molecules

The energy derivatives of valence shell MOs of selected heteronuclear molecules possessing 10 and 12 electrons in their valence shell are listed in Table 2. In addition to their symmetry, the MOs are labelled as n_X in relation to their main localization, in terms of "lone pairs". Chart 1 gathers the Lewis structures of the 10- and 12-valence electron species considered in the present study (Tables 1 and 2).

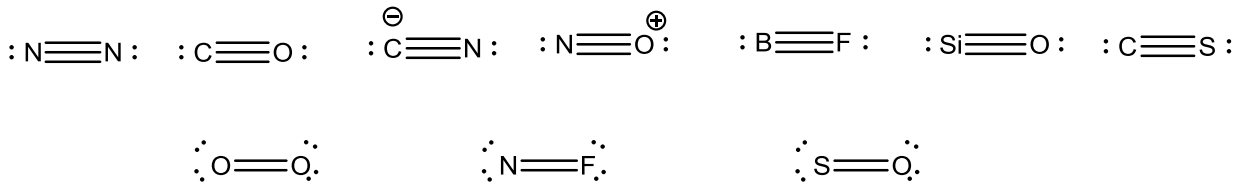


Chart 1

Table 2. Energy derivatives ε'_i (au) of valence MOs of selected heteronuclear diatomic species ((RO)HF/6-311G**) in their ground state; R_e (Å) experimental equilibrium distance; ΔR_e variation of the experimental equilibrium distance (Å) between neutral and cationic species in its ground state; in bold, ε'_i of the MO becoming singly occupied in the cation.

MO	CO	CO[a]	MO	CN^{-}[b]	MO	BF	MO	NO^+
3σ	0.377	0.299	**3σ**	0.232	**3σ**	0.293	**3σ**	0.592
4σ (n_O)	0.052	0.008	**4σ (n_N)**	**-0.114**	**4σ**	0.234	**4σ**	-0.053
π	0.242	0.184	**π**	0.136	**π**	0.208	**π**	0.317
5σ (n_C)	**-0.067**	**-0.048**	**5σ (n_C)**	**-0.038**	**5σ (n_B)**	**-0.068**	**5σ (n_N)**	**0.037**
R_e	1.128			1.177		1.267		1.063
ΔR_e	-0.013			-0.005		-0.057		0.034[g]
ΔR_e				-0.02[c]				

Table 2 (continued)

MO	SiO	MO	CS	MO	NF[f]	MO	SO[f]
5σ	0.176	**5σ**	0.186	**3σ**	0.373	**5σ**	0.296
6σ (n_O)	0.024	**6σ (n_S)**	-0.052	**4σ(n_F)**	0.042	**6σ (n_O)**	-0.032
3π	0.135	**7σ (n_C)**	**-0.049**	**1π**	0.217	**7σ (n_S)**	0.116
7σ (n_{Si})	**-0.016**	**3π**	0.104	**5σ(n_N)**	0.021	**3π**	0.249
				2π	**-0.146**	**4π**	**-0.101**
R_e	1.510		1.534		1.3170		1.4811
ΔR_e	0.006[e]		-0.034		-0.134[d]		-0.057

[a] B3LYP/6-311G** [b] 6-311+G** [c] loss of a 4σ electron.[d] Calc. value taken from NIST databank [e] Taken from ref. 20. [f] Triplet ground state. [g] Taken frome ref 19.

The following observations emerge from the above calculations. In the series of 10 valence electrons species, we note that: (a) in CO and in SiO, the n_O is bonding while the HOMOs n_C and n_{Si} are antibonding; in contrast, both n_C and n_S are antibonding in the analogous molecule CS; (b) in CN^-, both n_C (HOMO) and n_N are antibonding; (c) in BF, the n_B (HOMO) is antibonding; the 4σ MO is mainly located on fluorine, but cannot be viewed as a "lone pair" due to the strongly positive value of ε'_i. (d) In contrast to the other molecules of the same period, the lone pair n_N 5σ of NO^+ is found bonding, which agree with the bond lengthening observed in the dication NO^{2+}.[19] These results qualitatively agree with previous calculations by Bickelhaupt et al. of BP86/TZP σ MO energy derivatives in the series F_2, N_2, CO, BF, NO^+ and CN^-, with absolute values of ε'_i smaller by 10 % to 40 % than those reported here.[15]

The molecules NF and SO possess 12 electrons in their valence shell and have a triplet ground state, like O_2. Due to electronegativity difference of fluorine and nitrogen, NF possesses two MOs with a marked σ "lone pair" character (4σ and 5σ), both slightly bonding. The 7σ MO of SO is of n_S type with a bonding character (ε'_i = 0.116 au) close to that of the corresponding $3\sigma_g$ MO of O_2, while the oxygen lone pair (6σ) is slightly antibonding.

In all but one of these cases, the sign of ε'_i is in agreement with the bond length variation ΔR_e resulting from loss of the corresponding electron: whenever ε'_i is positive, ΔR_e is positive and *vice versa*. The only exception is SiO, for which the ionization from the weakly antibonding n_{Si} MO (ε'_i = -0.016 au) results in a slight lengthening (ca. 0.006 Å according to experimental result) [20] of the bond.

Bonding or antibonding "lone pairs" of CO and N_2.

The comparison of the isoelectronic species CO and N_2 is of special interest because N_2 is also able to act as a ligand in a variety of metal complexes. [21] Most textbooks [22] consider the MO $3\sigma_g$ (n_N) of N_2 as bonding and the HOMO 5σ (n_C) of CO as antibonding, in agreement with the

observed bond length variation upon ionization (Table 2). This result is further supported by the shortening of the CO bond upon protonation into H-CO^+ (see Table 6) [23]. Another experimental result in favour of the antibonding nature of the n_C MO is the observed ν(CO) stretching frequency in metal carbonyl complexes which is generally diminished by back donation from the metal into the π* MO of CO[17b] . In some electron-poor representatives, however, the σ-donation towards the metal (M←CO) overcomes the back donation (M⇉CO), leading to enhanced ν(CO) values. [24]

It should be emphasized that the (anti)bonding character of n_C of CO has been the subject of debate in the literature. For instance, taking the overlap population as a criterion, Radius e*t al*. [25] attribute an antibonding character to n_C of CO; the same conclusion has been drawn for n_N in N_2. On the other hand, comparing the perturbations of CO when H^+ (or a positive point charge Q) approaches either the carbon or the oxygen atom, Frenking et al. [26,27] take the opposite position with respect to the bonding character of n_C. These authors attribute the bond length variations of CO to perturbations of its π MOs, becoming more or less bonding as it gets more or less symmetrical. We have attempted to probe this issue in the present study, as described below.

Let's first study the sensitivity of the ε'_i criterion to the basis set and to the calculation methods. To do this, we consider the ε'_i values for several basis set HF calculations, EHMO and the semi empirical AM1 method in Table 3.

Table 3. Energy derivatives ε' (au) of MOs n_C of CO and n_N of N_2 and bond length variation ΔR_e at the same level of calculation (HF or DFT with the B3LYP functional)

	EHMO[a]	STO-3G	AM1	3-21G*	6-311G*	cc-pVTZ	cc-pVQZ	B3LYP[b]
n_C (CO)	-0.079	0.042	-0.051	-0.057	-0.067	-0.066	-0.067	-0.048
ΔR_e	-	0.060	-0.030	-0.007	-0.016	-0.017	-0.017	-0.017
n_N (N_2)	-0.095	0.135	-0.069	0.067	0.047	0.050	0.046	0.025
ΔR_e	-	0.099	-0.018	0.023	0.017	0.017	0.017	0.014

[a] with the HF/6-311G* value of R_e [b] 6-311G* basis set

Inspection of the results of Table 3 shows that ε'_i values converge for triple zeta or higher basis set quality (maximum variations of 0.001 au for n_C and 0.004 au for n_N). The HOMO of N_2 is $1\pi_u$, but the $3\sigma_g(n_N)$ is quasi-degenerate, about 0.01 to 0.02 au lower in energy. The results from 6-311G**/B3LYP Kohn-Sham MOs are in qualitative agreement with HF ones, though weaker in absolute value.

In contrast, the ε'_i values appear quite unreliable when computed with smaller basis sets or semi-empirical methods. For example, ε'_i is positive for n_C at the HF/STO-3G level while it is negative for n_N at the EHMO and AM1 levels. Interestingly, these "anomalous" results are consistent with the bond length of the ions calculated at the same levels. Indeed, at the HF/STO-3G level the CO bond is *longer* by 0.06 Å than in CO^+ than is CO whereas the NN bond length

calculated at the AM1 level is *shorter* by 0.02 Å in N_2^+ than in N_2. This comparison implies that when dealing with quasi non-bonding MOs, the bonding character may vary if calculated with a low quality method. It means that, if we refer to Figure 1, a small shift of the electron density from a bonding/antibonding area to another can be enough to change the sign of its force on nuclei.

Finally, based on ε'_i values shown in Table 3, the 5σ lone pair of CO is antibonding, whereas the $3\sigma_g$ one of N_2 is bonding, also in agreement with the additive orbital force calculations of Bader *et al.* [28] and results from Bickelhaupt.[15]

Figure 3 shows the continuous evolution of the characters of the valence shell MOs from CO to N_2 by using fictitious molecules with variable nuclear charges. The charge of "oxygen" nucleus is replaced by $8 - q$, down to 7 ($0 < q < 1$) and the charge of "carbon" nucleus by $6 + q$ up to 7. A basis set merging C and O 6-311G** atomic functions was used. The values of ε'_i are reported on Figure 3 as a function of q. We can see that the derivatives of the lower $3\sigma/2\sigma_g$ MO and the π MOs remain almost constant while the main evolution concerns the $4\sigma/2\sigma_u$ and $5\sigma/3\sigma_g$ MOs that exchange their bonding/antibonding characters. The bonding $3\sigma_g$ MO of N_2 becomes the 5σ antibonding one of CO (though there is no phase inversion between C and O nuclei), by a shift of electron density towards the antibonding zone nearby carbon (see Figure 3).

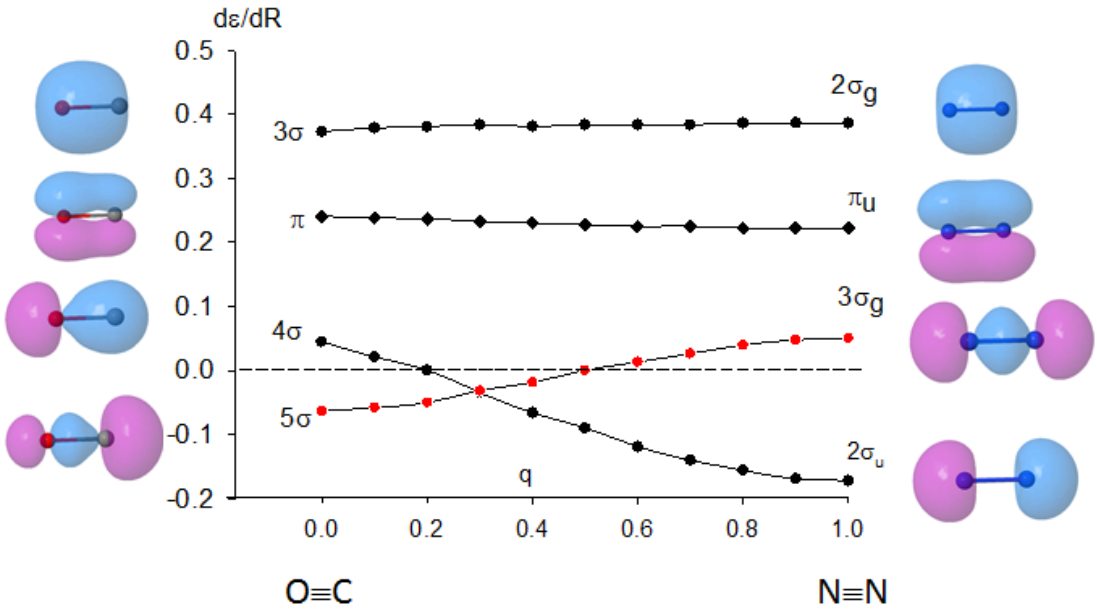


Figure 3. Evolution of dε/dR of valence MOs from CO to N_2 by variation of the nuclear charges 8 - q and 6 + q, as a function of q ($0 \leq q \leq 1$).

Case of HCN and HNC

Table 4 lists the calculated MO energy derivatives with respect to the C-H and C-N bond lengths of HCN and HNC. These calculations were performed by variation of one bond length, the other being kept constant. Examination of the values for HCN indicates that the 3σ MO is strongly

bonding along CN and 4σ is bonding along CH with a non-negligible antibonding character along CN. The 5σ MO, which is associated with the lone pair of nitrogen, is found to be slightly antibonding with respect to CN and only slightly bonding with respect to CH. From its graphical representation (Figure 4), this MO could appear as essentially bonding on both CN and CH bonds. However, this counter intuitive result can be qualitatively understood as follows. Dealing with CN, the two blue components of electron density are located in antibonding zones and overcome the bonding effect of the red one; dealing with CH, the red component has an antibonding effect which almost compensates the blue bonding component on this bond.

Table 4. Energy derivatives $d\varepsilon/dR_{CN}$ and $d\varepsilon/dR_{CH}$ (au) of valence MOs of HCN and HNC, with respect to C≡N and C-H bond lengths; HF/6-311G** level of calculation.

	H-C≡N			C≡N-H	
MO	$d\varepsilon/dR_{CN}$	$d\varepsilon/dR_{CH}$	**MO**	$d\varepsilon/dR_{CN}$	$d\varepsilon/dR_{NH}$
3σ	0.255	0.003	**3σ**	0.255	0.057
4σ	-0.077	0.209	**4σ**	0.068	0.232
5σ (n_N)	-0.030	0.017	**π**	0.182	0.025
π	0.170	0.008	**5σ (n_C)**	-0.111	0.021

Moreover, at first glance, it may be also surprising that the π MOs are found slightly bonding along CH ($d\varepsilon/dR_{CH}$ = 0.008 au), while their overlap is zero with the 1s OA of the H atom. It should be recalled, however, that i) the presence of p polarization basis functions on H allows a weak bonding interaction and ii) the π density exerts a non-zero force on the H nucleus. The same phenomenon is observed in HF and HCl, where the p lone pairs of F and Cl have a positive ε'_i (0.055 au and 0.013 au, respectively), in agreement with the observed lengthening of these bonds in the $^2\Pi$ ground state of cations HF^+ and HCl^+ (0.084 Å and 0.04 Å respectively). These results are also supported by orbital force calculations. [29,30] From Figure 2, it is clear that the 2p density on the fluorine atom in HF is not equally spread in the bonding and antibonding regions. Indeed, it is difficult to predict whether this force is attractive or repulsive.

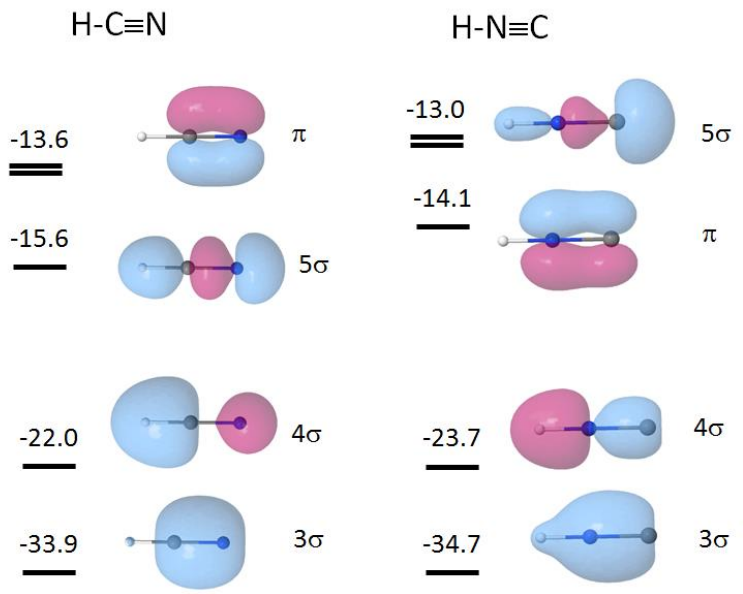


Figure 4. Valence shell MOs of H-CN and H-NC (only one of each π degenerate set has been reported; energies in eV; HF/6-311G** level of calculation).

The MO diagram of HNC exhibits some differences as compared to that of HCN. First, the 5σ, formally a carbon lone pair, is now the HOMO and becomes more antibonding on CN, in contrast to what was observed in HCN. Second, the 4σ becomes slightly bonding on CN. Again, the π MOs are found to have a bonding character along NH ($d\varepsilon/R_{NH}$ = 0.025 au) though their overlap with the valence 1s MO of hydrogen is zero.

Acetonitrile CH_3CN

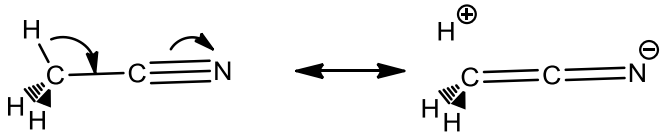
The bonding character of the nitrogen lone pair of nitriles is of interest in order to study their coordination chemistry. In Table 5, we report MO energy derivatives of CH_3CN with respect to each bond length, all other internal coordinates being kept constant, with 6-311G** and cc-pVQZ Dunning's basis sets.

These data allow us to attribute the character(s) of each MO with respect to each bond, and do so more readily and confidently than by simple visual examination (cf. Figure 5). The $7a_1$ MO (HOMO - 2) essentially describes the lone pair of nitrogen; it is antibonding along CN (-0.010 au and -0.015 au according to the basis set). This antibonding character is weak as compared to that of the HOMO of CO (-0.07 au) and also weaker than that of the corresponding MO of HCN (-0.03 au). The $6a_1$ MO, which is more strongly antibonding along CN and bonding along CC and CH, possesses also a small lobe pointing from nitrogen.

Table 5. Energy derivatives $d\varepsilon/dR_{XY}$ (au) of valence MOs of CH_3CN with respect to their bond lengths (a) HF/6-311G** (b) HF/cc-pVQZ.

MO	$d\varepsilon/dR_{CN}$		$d\varepsilon/dR_{Cc}$		$d\varepsilon/dR_{CH}$	
	(a)	(b)	(a)	(b)	(a)	(b)
$4a_1$ (σ_{CN})	0.255	0.249	0.010	0.010	-0.004	-0.002
$5a_1$ (σ_{CH})	-0.023	-0.025	0.111	0.111	0.146	0.147
$6a_1$ (σ_{CC})	-0.069	-0.071	0.081	0.081	0.068	0.069
1e (π_{CH})	-0.004	-0.006	0.041	0.042	0.147	0.148
$7a_1$ (n_N)	-0.010	-0.015	0.008	0.007	-0.004	-0.003
2e (π_{CN})	0.157	0.156	-0.029	-0.029	0.014	0.015

It is worth noting that the 1e MOs associated with CH_3 bonds ($d\varepsilon/dR_{CH} \approx 0.15$ au) are also bonding along CC ($d\varepsilon/dR_{CC} \approx 0.04$ au) and slightly antibonding along CN ($d\varepsilon/dR_{CN}$ = -0.004 - -0.006 au) in agreement with the classical scheme of hyperconjugation:



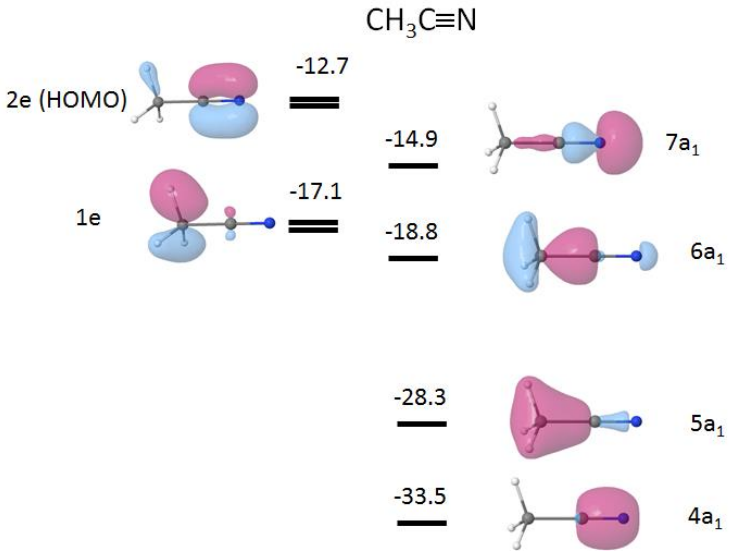


Figure 5. Valence shell occupied MOs of CH_3CN (energy in eV; only one of each degenerate set has been reported; HF/6-311G** level of calculation).

Canonical MO energy derivative: a reliable criterion of bonding character

From the results of Tables 3 and 5 obtained with various basis sets, it is reasonable to conclude that ε'_i, calculated with a triple zeta quality basis set, is a reliable parameter associated with each MO. Note that the differences in ε'_i values calculated with various TZ and QZ basis sets are no more than 0.002 au in most cases, with a maximum of 0.006 au. In other words, the uncertainty on these results is about 0.005 au in absolute value.

From Tables 1 and 2, it has been shown that the sign of ε'_i allows the prediction of the effect of ionization from the i^{th} spin orbital on the bond length: when $\varepsilon'_i > 0$, the bond length increases, which is consistent with a bonding MO in the sense of Mulliken. Moreover, a correlation is found between ε'_i and the experimental relative bond length variation, as long as this variation is small (< 10 %). This correlation, shown in Figure 6, includes the results of Tables 1 and 2 (except H_2 and Li_2), HF and HCl.

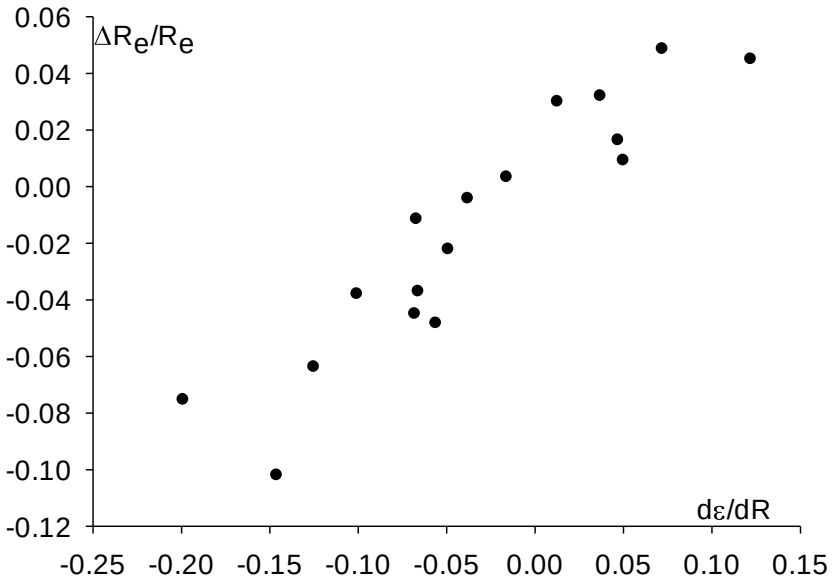


Figure 6. Experimental relative variation $\Delta R_e/R_e$ of the bond length by ionization, as a function of the MO energy derivative $d\varepsilon/dR$ (au) of the removed electron, in a series of diatomic molecules (HF/6-311G**).

There is indeed a continuum from strongly bonding to strongly antibonding MOs (strictly non-bonding MOs, with $d\varepsilon/dR = 0.0000...$, are theoretical situations of negligible occurrence in the molecular realm). Nevertheless, we can propose rough landmarks for the bonding characteristics of MOs of diatomic molecules. In second period diatomic molecules, a mean ε' value of ca. 0.30 au is found for σ bonding MOs and 0.20 for π bonding MOs; absolute values of ε' less than 0.1au refer to essentially "non-bonding" MOs. These values are divided by about 3 when dealing with third period diatomic molecules whose bonds are significantly weaker, and by about 1.5 for

molecules mixing these both elements. In polyatomic molecules, such a classification becomes difficult because several MOs may contribute almost equally to the same bond (see Table 5).

Perturbation by electron acceptors: protonation, proton interaction and effect of an electric field

Protonation.

In addition to the complete removal of an electron, the experimental consequences of a partial electron transfer from a MO to an electrophile are possibly rationalized from the bonding/antibonding nature of this MO. The simplest electrophile is H^+, which can be viewed as the simplest model of a metal centre, and one could assume that the main effects of protonation can be predicted according to the character of the lone pair to be protonated. For a bonding lone pair, electron density is partly removed: a lengthening of the bond and other effects qualitatively similar to ionization are generally expected. It is clearly visible for seven of the eight entries of Table 6.

Table 6. Values of $\varepsilon'_i = d\varepsilon_i/dR_{XY}$ (au) of the lone pair in the free molecule X≡Y and experimental variation ΔR_{XY} (Å) of XY bond length by protonation; ($(HCNH)^+$ can be considered either as protonated HCN or as protonated HNC).

R-H$^+$	$^+$H-C≡O	C≡O-H$^+$	N≡N-H$^+$	H-C≡N	C≡N-H	HC≡N-H$^+$	$^+$H-C≡NH	CH_3C≡N-H$^+$
ε'_i	-0.067	0.052	0.047	-0.114	-0.038	-0.030	-0.111	-0.010
ΔR_{XY}	-0.023[a]	0.029[a]	-0.005[b]	-0.021	-0.004	-0.070[c]	-0.035[c]	-0.011[d]

[a]From ref. 23; [b] From ref 32; [c] From ref. 31; [d] Calculated value (B3LYP/6-311G**)

As anticipated, the protonations on each side of CO have opposite effects on the C-O bond length, [23] in agreement with the opposite characters of the corresponding lone pairs. In contrast, both protonations of CN^- shortens the CN bond [31], in agreement with the antibonding character of both C and N lone pairs. For N_2, we observe that the protonation slightly shortens the NN bond [32], in contrast to the ionization. This can be understood by considering that, due to the symmetry of N_2, the protonation withdraws electrons as well from the bonding $3\sigma_g$ as from the antibonding $2\sigma_u$ (see Fig. 3).

Proton approach and electric field.

Goldman and Krogh-Jesperson have argued that the increase of the force constant of CO in cationic complexes can be essentially described by an electrostatic effect (exerted by a point charge), and not by σ-donation from an antibonding MO. [33] In fact, from a force point of view, these phenomena result in pulling electron density from the ligand towards the cation, and could appear as closely related. Nevertheless, we will examine below the impact on CO and CH_3CN of an approaching proton and of embedding these molecules into an electric field (which can be

actually considered homogeneous if exerted by a sufficiently remote and high point charge on the bond axis).

In Figure 7, we report the MO energy derivatives of CO when a proton is approached to carbon or oxygen atom. In both cases, the derivatives of the energies of 3σ (σ_{CO}) and π MOs increase slightly. In contrast, the MOs 4σ and 5σ associated with the C and O lone pairs are strongly perturbed. When H^+ approaches the carbon atom, n_C becomes less antibonding and finally slightly bonding, whereas n_O becomes less bonding an finally antibonding. When H^+ approaches the oxygen atom, these trends are qualitatively strictly inverted.

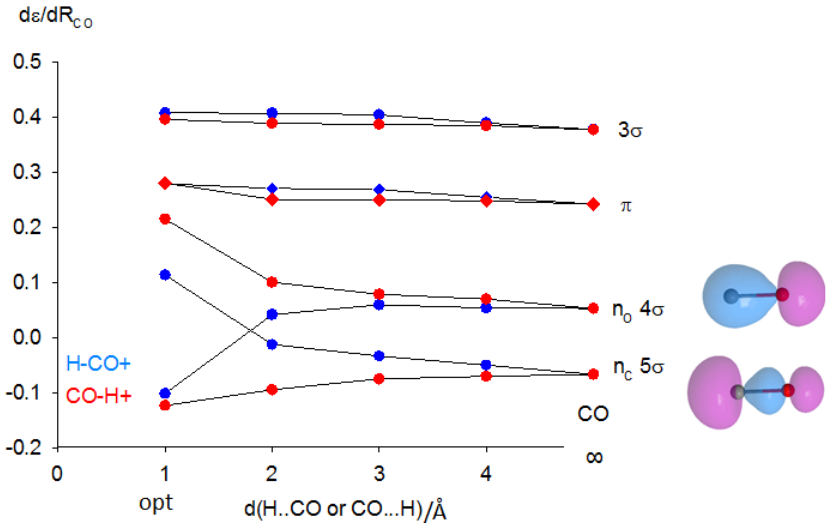


Figure 7. MO energy derivative dε/dR_{CO} (au) for H^+…CO (blue) and CO…H^+ (red) at various H…C (resp. O…H) *d* distances (Å) and optimized (opt) geometry.

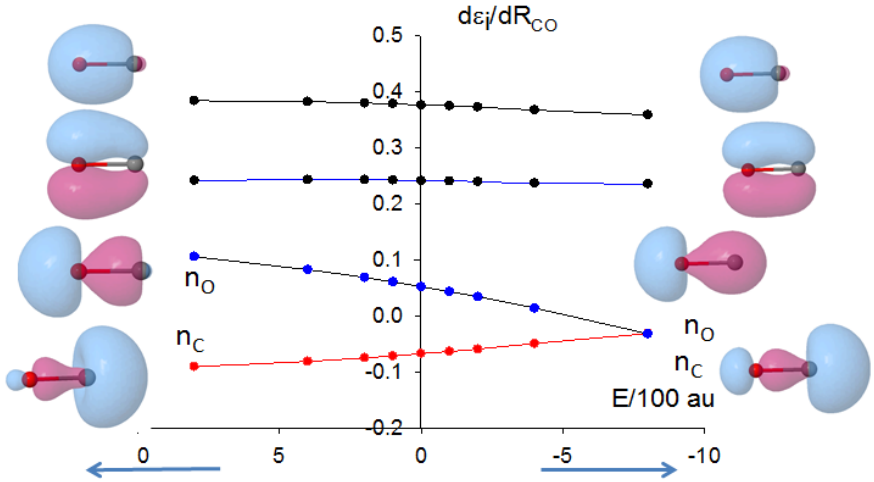


Figure 8. Effect of an electric field *E* on MO energy derivatives dε/dR_{CO} (au) of CO. The arrows indicate the direction of electron shift.

The effect of an electric field appears to be quite similar to proton approach (Figure 8). Thus in the left segment on the Figure 8 (positive field) the electrons are shifted from oxygen to carbon, which corresponds to red points in Figure 7 (CO…H^+). We observe that the ε' of π MOs undergo relatively small variations even though they are significantly distorted. We observe also a divergent variation of ε' for n_C and n_O.

The right segment of Figure 8 (negative field) corresponds to electron shift from carbon to oxygen (cf. blue points H^+…CO approach in Figure 7). It results in a convergent variation of ε' of n_C and n_O. To these monotonous variations corresponds a monotonous variation of the calculated CO vibration frequency and bond length (see Figure 9 and 10) which follow the energy derivative of the HOMO n_C, despite the decreasing bonding character of n_O. The variation of ν_{CO} suggests that a maximum of frequency should be reached for a field value of ca. 0.1 au, in agreement with previous reports. [34]

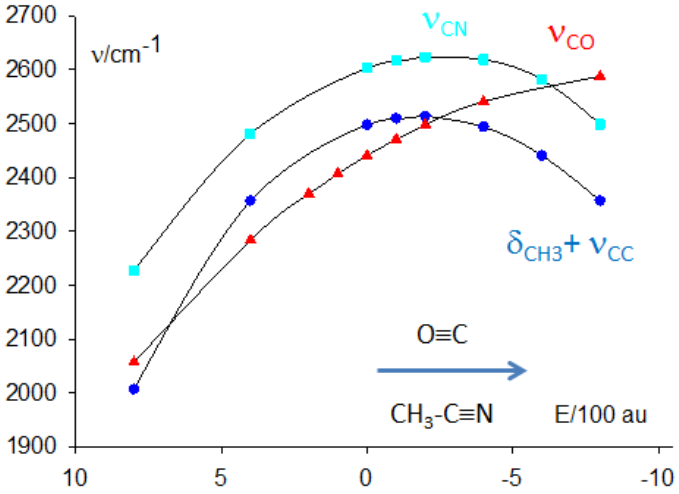


Figure 9. Calculated vibration (HF/6-311G*) frequencies of CO and CH_3CN as a function of electric field E oriented along molecular axis; the arrow indicates the direction of electron shift for $E < 0$.

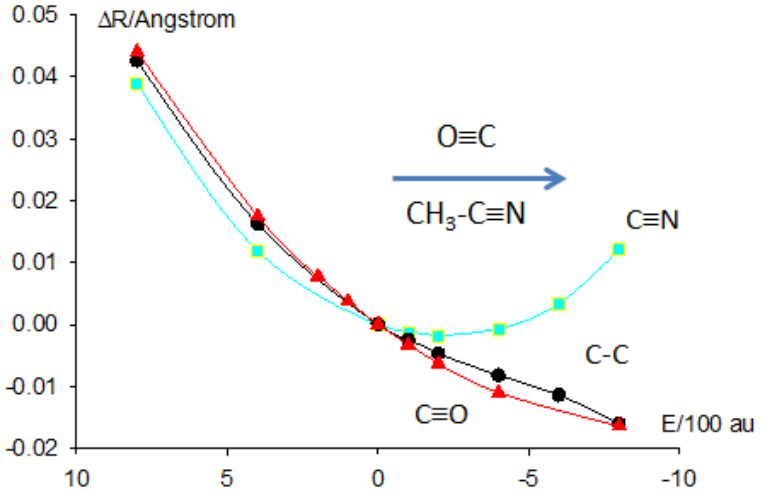


Figure 10. Variation of bond lengths ΔR (Å) in CO and CH_3CN as a function of electric field E oriented along the molecular axis; the arrow indicates the direction of electron shift for $E < 0$.

The situation is quite different when we consider CH_3CN, as displayed in Figure 11. When a proton approaches the nitrogen atom, the bonding character along CN of most of the MOs is noticeably perturbed, especially $4a_1$ (σ_{CN}) and both e (π) MOs. Also, the variation of $d\varepsilon/dR_{CN}$ of $7a_1$ (nitrogen lone pair) $5a_1$ and $6a_1$ is no longer monotonous.

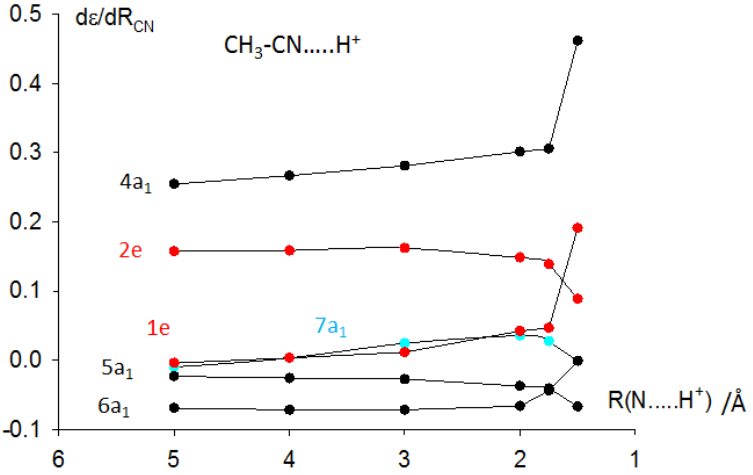


Figure 11. MO energy derivative $d\varepsilon/dR_{CN}$ (au) for $CH_3CN...H^+$ at various $N\ldots H^+$ distances (Å).

The effect of an electric field (Figure 12) gives a deeper insight on these phenomena especially in the region of negative field (electron shift from C to N); a crossing occurs between the two sets of π MOs which exchange their bonding characters on CH_3 and CN. These dramatic changes arise from the high polarizability of the π hyperconjugated system, as compared with CO (the

dipole moment is increased by 7.5 D for CH_3CN and 2.8 D for CO by a field of 0.08 au). As with the proton approach, the energy derivative of the $7a_1$ lone pair reaches a maximum bonding for a field value of ca. -0.04 au.

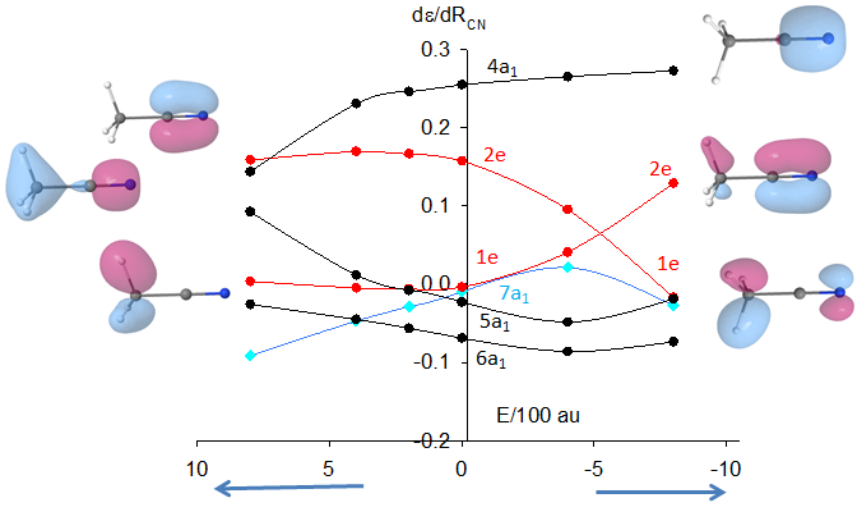


Figure 12. Effect of an electric field *E* on MO energy derivatives $d\varepsilon/dR_{CN}$ (au) in CH_3CN. The arrows indicate the direction of electron shift.

Figure 9 shows the variation of calculated vibrational frequencies of CH_3CN as a function of the electric field E. The CN frequency does not vary monotonously in the electric field range considered and a maximum positive shift is observed at ca. 20 cm^{-1} for a field of ca. -0.025 au with respect to free acetonitrile at zero field. The same order of magnitude of these values (20-30 cm^{-1}) is observed experimentally [35,36], though in some cases much higher values have been measured [17c,d]. The equilibrium bond length of CN is minimal at about the same value of the electric field (Figure 10). It is remarkable that these extrema also occur at about the same field value as the maximum of ε' of the lone pair $7a_1$. Nevertheless, this result must be considered with caution, because other MOs undergo strong variations in their bonding character and in opposite directions. Furthermore, the frequencies of free CH_3CN at 2252 and 2293 cm^{-1} are attributed to a Fermi resonance between the fundamental ν_{CN} and the combination ($\nu_{CC} + \delta_{CH3}$). These fundamental vibrations themselves involve the participation, in their normal coordinate, of other vibrators which are also strongly perturbed by an electric field as it can be seen in Figure 9. Yet, Table 5 suggests that the $7a_1$ MO, as well as $6a_1$, antibonding along CN, should have also a noticeable bonding character along CC. Indeed, the CC bond is found shorter in the presence of proton or electric field and decreases monotonously with the electric field (Figure 10).

Conclusion

Our results have shown that, on the basis of the Koopmans theorem, the derivative ε'_i of the energy of a canonical MO ϕ_i with respect to the distance *R* between two nuclei A and B can be

considered as a good index of the bonding/antibonding character of this MO along A-B. Thus, the sign of ε'_i allows the prediction of the sign of variation of the bond length A-B of diatomic molecules by ionisation, which is itself a criterion of the bonding character. The same conclusion generally holds for the effect of protonation on the bond length. These derivatives can be easily computed and their results can be extended to any geometrical deformation of a polyatomic molecule. On this basis, the HOMOs $3\sigma_g$ of N_2 and 5σ of NO^+ are found to be bonding, whereas the HOMO 5σ of CO is found to be antibonding. The lone pairs of BF, CS, CN^-, HCN, HNC and CH_3CN are also more or less antibonding. In polyatomic molecules, where MOs are generally delocalized on several centres, the derivatives ε'_i with respect to each bond length indicate the relative bonding (or antibonding) contribution of the ϕ_i MO to this bond.

We have modelled the coordination to a cationic metal centre either by proton interaction or by embedding the ligand into an electric field. The results presented here support the current idea that qualitative predictions of bond length and vibration frequency variations of ligands can be done by considering the bonding/antibonding character of MOs mainly interacting with the metal, provided the ligand is a diatomic molecule such as CO. In other cases, like CH_3CN, several MOs are perturbed upon complexation, resulting in balanced effects on bond strengths and on the corresponding vibrators much or less coupled in the normal coordinates.

Moreover, canonical MOs are defined within HF approximation and their explanatory power is thus *a priori* restricted to phenomena correctly depicted, at least qualitatively, at this level of calculation.

We believe that these results open broad perspectives for experimentalists interrogating the nature of the bonding between acceptor and donor partners, especially in the field of coordination chemistry, where the nature of M-L bond is of particular significance. [37] It would be of primary interest to examine how the bonding/antibonding character of MOs of a given ligand is affected upon coordination to a 'real' metal centre, and the possible back-donation of the metal towards the ligand may interfere.

KEYWORDS: Molecular orbitals, bonding criterion, donor-acceptor interaction, diatomic molecules, acetonitrile.

References and Notes

[1] IUPAC. Compendium of Chemical Terminology, 2nd ed. (the "Gold Book"). Compiled by A. D. McNaught and A. Wilkinson. Blackwell Scientific Publications, Oxford (1997). XML on-line corrected version: http://goldbook.iupac.org (2006-) created by M. Nic, J. Jirat, B. Kosata; updates compiled by A. Jenkins. ISBN 0-9678550-9-8.

[2] R. Chauvin et al., work in progress

[3] a) J.S. Dewar, *Bull. Soc. Chim. Fr.* **1951**, *18*, C71–C79; b) J. Chatt, L. A. Duncanson, *J. Chem. Soc.* **1953**, 2939–2947; c) J. Chatt, L. A. Duncanson, L. M. Venanzi, *J. Chem. Soc.* **1955**, 4456–4460.

[4] T. J. Berlin, *Chem. Phys*. **1951**, *19(2),* 208-213.

[5] R. F. Bader, W. H. Henneker, P. E. Cade, *J. Chem. Phys.* **1967**, *46*, 3341-3363.

[6] T. Tal, J. Katriel, *Theoret. Chim. Acta* **1977**, *46,* 173-181.

[7] T. Koopmans, *Physica* **1934***, 1*, 104–113

[8] R. S. Mulliken, *Phys. Rev*. **1928**, *32*, 186-222.

[9] Y. Yamaguchi, R.B. Remington, J. F. Gaw, H. F. Schaefer III, *Chem. Phys*. **1994**, *180*, 55-70.

[10] Y. Yamaguchi, R.B. Remington, J. F. Gaw, H. F. Schaefer III, G. Frenking, *J. Chem. Phys.* **1993**, *98 (11)*, 8749-8760.

[11] Y. Yamaguchi, B. J. DeLeeuw, C. A. Richards, Jr., H. F. Schaefer III, G. Frenking, *J. Am. Chem. Soc.* **1994**, *116*, 11922-11930.

[12] A. Gobbi, Y. Yamaguchi, G. Frenking, H. F. Schaeffer III, *Chem. Phys. Lett.* **1995**, *244*, 27-31.

[13] H.Y. Lee, S.P. Wang, T.C. Chang, *Int. J. Quant. Chem*. **2001**, *81*, 53-65

[14] F. W. Averill, G. S. Painter, *Phys. Rev. B* **1986**, *34(4),* 2088-2095.

[15] F. M. Bickelhaupt, J. K. Nagle, W. L. Klemm *J. Phys. Chem. A* **2008**, *112*, 2437-2446

[16] P. J. Robinson, A. N. Alexandrova, *J. Phys. Chem. A* **2015**, *119*, 12862−12867

[17] a) J. H. Choi, K. I. Oh, H. Lee, C. Lee, M. Cho, *J. Chem. Phys.* **2008**, *128*, 134506(1)-134506(8); b) D. G. Gusev, *Organometallics* **2009**, *28*, 763-770; c) B. Vabre, Y. Canac, C. Lepetit, C. Duhayon, R. Chauvin, D. Zargarian, *Chem. Eur. J.* **2015**, *21*, 17403-17414; d) S. Lapointe, B. Vabre, D. Zargarian, *Organometallics* **2015**, 34, 3520-3531.

[18] Gaussian 09, Revision A.01, M. J. Frisch *et al*. Gaussian, Inc., Wallingford CT, 2009.

[19] D. Cossart, C. Cossart-Magos, J. Mol. Spectrosc. 1991, 147 471-477

[20] D. Shi, W. Li, W. Xing, J. Sun, Z. Zhu, L. Liu, *Comp. Theor. Chem*. **2012**, *980*, 73–84.

[21] a) T. Yamabe, K. Hori, T. Minato, K. Fukui, *Inorg. Chem*. **1980**, *19*, 2154-2159 b) M. D. Fryzuk, S.A. Johnson, *Coord. Chem. Rev*. **2000**, *200-202*, 379-409.

[22] a) T. A. Albright, J. K. Burdett, M.-H. Whangbo, *Orbital Interaction in Chemistry*, John Wiley & Sons, New York, **1984**, pp 78-82; b). F. A. Cotton, G. Wilkinson, *Advanced Inorganic Chemistry, 5th ed*.; John Wiley & Sons, New York, **1988** ; pp 58-64; c) R. H. Crabtree, *The*

Organometallic Chemistry of the Transition Metals, 2nd ed.; John Wiley & Sons: New York, **1994**; pp 13-15.

[23] N. L. Ma, B. J. Smith, L. Radom, *Chem. Phys. Lett.* **1992**, *197* (6), 573-580.

[24] A. J. Lupinetti, S. H. Strauss, G. Frenking, In *Progress in Inorganic Chemistry*, Vol. 49; Karlin, K. D., Ed.; Wiley, New York, **2001**, pp. 1-49.

[25] U. Radius, F. M. Bickelhaupt, A. W. Ehlers, N. Goldberg, R. Hoffmann, *Inorg. Chem.* **1998**, *37*, 1080-1090.

[26] G. Frenking, C. Loschen, A. Krapp, S. Fau, S.H. Strauss, *J. Comput. Chem*. **2007**, *28*, 117–126.

[27] A. J. Lupinetti, S. Fau, G. Frenking, S. H. Strauss, *J. Phys. Chem. A* **1997**, *101*, 9551-9559.

[28] R. F. W. Bader, A. D. Bandrauk, J. *Chem. Phys*. **1968**, *49*, 1653-1665.

[29] R. F. W. Bader, J. Keaveny, P. E. Cade, *J. Chem. Phys*., **1967**, *47*, 3381-3402.

[30] P. E. Cade, R. F. W. Bader, W. H. Henneker, I. Keaveny, *J. Chem. Phys*. **1969**, *50*, 5313-5333.

[31] C. E. Cotton, J. S. Francisco, W. Klemperer, *J. Chem. Phys*. **2013**, *139*, 014304.

[32] J. C. Owrutsky, C. S. Gudeman, C. C. Martner, L. M. Tack, N. H. Rosenbaum, R. Saykally, *J. Chem. Phys.* **1986**, *84*, 605-617.

[33] A. S. Goldman, K. Krogh-Jespersen, *J. Am. Chem. Soc*. **1996**, *118*, 12159-12166

[34] N. S. Hush, M. L. Williams, *J. Mol. Struc*. **1974**, *50*, 349-368.

[35] S. Liang, H. Wang, T. Deb, J. L. Petersen, G.T. Yee, M.P. Jensen, *Inorg. Chem*. **2012**, *51*, 12707−12719.

[36] W.E. Buschmann, J. S. Miller, *Chem. Eur. J*. **1998**, *4*, 1731−1737.

[37] C. Lepetit, V. Maraval, Y. Canac, R. Chauvin, *Coord. Chem. Rev*. **2016**, *308 II*, 59-75.